A Review of Basic Concepts in Comprehensive Two-Dimensional Gas Chromatography

Ruby C.Y. Ong and **Philip J. Marriott***

Centre for Chromatography and Molecular Separations, Royal Melbourne Institute of Technology, GPO Box 2476V, Melbourne, 3001, Australia

Abstract

The technique of comprehensive two-dimensional gas chromatography (GC×GC) is reviewed. A description of technical aspects of the method illustrates how the GC×GC result is achieved through the use of dual-coupled columns and the modulation of capillary chromatographic peaks. This review presents an expanded section dealing with the relationship between the modulation phase and frequency and the resulting peak pulse profiles. Experimental results that support the appreciation and understanding of the effects that pulsing has on a chromatographic peak are provided. The main goals of GC×GC analysis are discussed with respect to analytical sensitivity and peak capacity arising from zone compression effects and fast analysis on the second column. A typical application of GC×GC is presented, along with a consideration of implementation of the GC×GC method.

Introduction

Comprehensive two-dimensional gas chromatography (GC×GC) is now a well-established (albeit relatively new) operating method for high-resolution gas chromatography (GC). A recent review illustrates the conceptual framework, technical implementation, and potential scope of the technique (1). Its often-stated benefits include enhanced sensitivity (2,3) and superior resolution (4), which arise from the process of compressing the eluting chromatographic band in a modulation region at the end of a first-dimension column and using a fast-elution (usually short) second-dimension column between the modulation region and the detector to which the compressed zone is rapidly introduced. Davis (5) discussed the need for increased resolution power arising from GC×GC. GC×GC arises from the pulsing of solute emerging from one column (the primary column) into a second column, with the time period of pulsing shorter than the primary column peak-elution duration. The process is aided by the use of a modulation device at the column junction; a number of different modulators have been described. The history of GC×GC dates from work in the early 1990s (6); however, a reliable modulation of chromatographic signals was not achieved until relatively late in the decade. The most important outcome of GC×GC has been the great increase in the peak capacity of the GC experiment. This has two major benefits. First, for a complex sample it is possible to present many more peaks in a chromatogram, because of expansion in the available separation space. Second, and this is an outcome of the first, specific problem separations may now be resolvable in ways that have previously been either difficult or impossible.

It is necessary when discussing multidimensional or comprehensive chromatography to acknowledge the contributions of Giddings (7) and Schomburg (8), who both expounded on the potential power that lay at the heart of coupled column chromatography and thoroughly investigated the experimental implementation of conventional multidimensional GC (MDGC) in many different modes. However, although a relatively easy mental association between what is now recognized as GC×GC and the conceptual writings of Giddings can now be made, it was Phillips who tackled this task experimentally and showed that by suitable technical innovation it should be possible to realize the result that Giddings could only dream of. Today, experienced users of GC×GC with reproducible and relatively simple modulation systems at their disposal might wonder why there was such a difficult and lengthy gestation period before the results that are now taken for granted could be reliably generated. Even over the past few years, it might be wondered why there was not an avalanche of interest in GC×GC. Impressive results were demonstrated at least five years ago, and the frustrations of trying to convince chromatographers of the worth of the tool were running high. The reason may be that most were just overawed by what they were being shown with literally thousands of separated components in the 2D space. However, one needs to look only to high-resolution electrophoresis separations of proteins to know that there were a number of separation scientists who were already dealing with equally challenging 2D results. It will be left to other forums to try to decide the reasons for the slow take up of GC×GC.

Today, GC×GC has an established foothold in both the literature and scientific meetings, albeit still in an infancy stage. As the uptake of GC×GC occurs in a wider range of laboratories and its use for a more diverse application base continues to expand, then the pressure will build for an even greater validation of GC×GC methodologies for practical solutions to chromatographic prob-

* Author to whom correspondence should be addressed: email philip.marriott@rmit.edu.au.

lems. This challenge is laid squarely at the feet of the pioneers of GC×GC.

This study will provide an overview of the basics of GC×GC and draw on our various experiences and those of other laboratories to describe the fundamentals and current state of GC×GC studies.

Technical implementation of GC×GC

GC×GC methodologies require a "total systems" development (which is the radical way that capillary GC×GC alters the practice and conduct of GC analysis) to the extent of even demanding new thought processes on the part of the chromatographer compared with conventional single-column GC and MDGC. Some of these will be outlined.

Modulator considerations

Modulators based on temperature differences. The modulator serves to allow the chromatographic peak that elutes or emerges from the end of the primary column to be time-sampled into the second column. Lee et al. (9) recently reviewed a number of technologies used for modulation; however, such is the pace of development that other modulators have since been reported. Figure 1 summarizes in schematic form a range of modulators that have been described. Most modulators operate under conservation of mass principles, such as the thermal and cryogenic modulators. These modulators rely on some measure of the focusing or slowing of the migration of the chromatographic peak. The principles of cryogenics in GC are well-known, because a cool region will readily trap the volatile compounds. However, the thermal modulator must incorporate a means to reduce the speed of the migration of the peak, and this was achieved by incorporating a thicker film column at the modulation region. This increases the component retention factor (k) and retards its travel. The thermal modulator then uses an application of high temperature to rapidly flush that zone of compound out of the modulator region and deliver it to column 2.

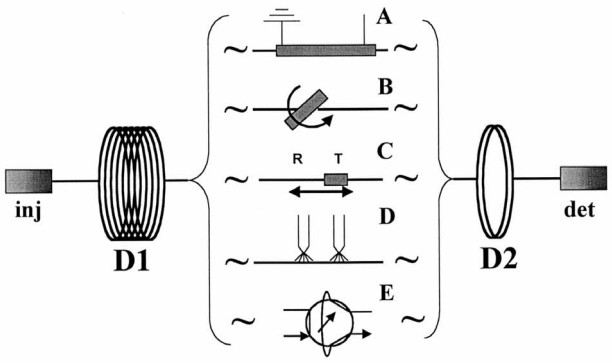

Figure 1. Schematic diagrams of various modulators used for GC×GC that collect or trap solute coming from the primary dimension (D1) and pulses it to the second dimension (D2): (A) a heated tube encasing the capillary column (the first example of this was that of a metal paint-coated column, a supplementary electrical supply was used to heat the metal); (B) the thermal sweeper system with a rotating slotted heater sweeping over the accumulation column and column connections to collect and pulse solute to the second column; (C) the LMCS that uses an oscillating cryotrap to trap the solute peak (position T), thus allowing it to heat up and remobilize by moving to the release position (position R); (D) a dual jet modulator using two jets to supply localized cryogenic cooling to the column; and (E) an example of the valve system that partially fills a loop and then switches the valve to flush the loop to the second column (the diagram shows the valve in the flush position).

The first thermal modulator was comprised of a metal-coated length of column (Figure 1A) that could be thermally cycled by electrical means; however, it suffered from breakdown of the coating and was unreliable. The second thermal modulator (also termed the thermal sweeper) used a rotating slotted heater to sweep over the modulator column to push solute towards column 2 (10) (shown in abbreviated form in Figure 1B). This modulator suffered from reliability problems early in its development and may have been tedious to set up (requiring uncoated column sections, up to four column connections, and careful adjustment of column dimensions); however, it was also reported to be robust (11). The need to use elevated temperatures to remobilize the retarded solute (approximately 100°C above the oven temperature) leads to a natural temperature limit for oven operation. It seems at present that this modulator has lost favor and is being replaced by other modulation mechanisms.

The first cryogenic modulator, the longitudinally modulated cryogenic system (LMCS) (Figure 1C), was developed by us and initially described as a means to focus whole peaks just prior to a detector and provide enhanced sensitivity. Since then, a range of other operational modes have been described, such as targeted MDGC. This modulator collects and concentrates a segment of the chromatographic band that enters the cryogenic trap region and by moving the modulator along the column exposes the cryotrapped solute to the oven heat, thereby allowing the solute to be rapidly mobilized and travel down the second column. Thus, the trap can be used to collect whole peaks or modulate contiguous segments of a peak.

More recently, two different cryogenic jet modulators have been studied, with one design simply pulsing the cryogenic jets on and off (Figure 1D). With the jets placed longitudinally along the column (upstream/downstream), they perform in a similar process as the LMCS, ensuring that when the second jet is turned off there is no breakthrough of solute passing through the cryotrapping region (12). The other cryogenic jet modulator provides a supply of hot gas to heat the cold region and allow for the mobilization of solute (13). It should be noted that the thermal sweeper has been modified by some users to incorporate supplemental improved trapping performance such as by using an independently controlled temperature to allow the accumulator column to be operated at a lower temperature to reduce solute breakthrough (14). The same effect can be achieved by the use of a jet of cryogen applied to the outer column wall, with the sweeper arm interrupting the cryogen flow to the column when the column heating stage is activated.

Modulators based on valve operation. Other modulator designs sample less than the complete chromatographic peak, such as the diaphragm modulator of Synovec (15), in which maybe only 5% of the band is transferred to the second column. Because this can operate at a relatively high frequency, it can be used for very fast peaks. The transferred band is not compressed but may have a bandwidth of as small as 10 ms. By comparison, the valve system of Seeley (16) (as depicted in Figure 1E) would appear to almost achieve full mass transfer to the second column. In this instance, a sampling valve is used to collect

solute coming from the end of the primary column into a collection loop, then upon switching the valve and backflushing the sampling loop into the second column at a very high flow rate, fast GC is achieved with a fast sample flux into the detector. The key to this method is the relative flow rates of carrier gas in each section (e.g., 0.75 and 15 mL/min, respectively).

It should be noted that all of these designs essentially are capable of generating the same sort of GC×GC result with data transformation that give sample peaks spread over a 2D separation space. It may be that certain modulators will be found to have specific benefits for selected analyses (e.g., for more volatile samples or high-temperature operation), which will become more apparent as further applications are studied.

Column considerations

Phase selection. The choice of which column phases to use in the two-column experiment is governed by the need of whether to achieve maximum component separation for a particular sample. This may be interpreted in terms of the columns' "orthogonality" (17), which is intended to maximize the difference in the columns' separation mechanisms with respect to the chemical components that are to be separated. The "normal" combination for the column set appears to be a nonpolar column followed by a polar (more selective) phase. The rationale for this is that the first column separates according to dispersive forces (with solutes presented at the end of the first column according to their boiling points), thus coeluting components may have a wide range of polarities. The second column then is chosen to enhance the separation of these when they are pulsed to column 2. In the reverse geometry, a nonpolar second column may be less effective in resolving different polarity solutes, and dispersive forces alone may be insufficient to provide effective resolution.

It is possible to use a more selective phase in the primary column, followed by the less selective. This was the case for polychlorinated biphenyl (PCB) analysis on a liquid-crystal-phase first column (18). It should be pointed out that it may still be a matter of trial and error in the selection of a column set, although some logical choices can easily be made. For instance, for petroleum products a low polarity phase (e.g., a 5%-phenyl-polysiloxane-type column, which is often used in single-column analysis) coupled with a high-percent phenyl phase is a good choice. This is because the purpose of the separation is to achieve the resolution of saturated compounds from coeluting unsaturated/aromatic compounds. A high-percent phenyl phase is good for this, because π–π interactions will selectively retain aromatics on the second column compared with alkanes and cyclic alkanes, which may coelute from the primary column. Interestingly, similar logic was used to decide on the column set for an atmospheric organic analysis in which the aromatic content of the sample was of interest (19).

In an attempt to predict the relative positions of fatty-acid methyl esters in the 2D space, the use of retention indices on each of the two columns to be used for GC×GC was modeled and applied to the GC×GC case (20). The results were not sufficiently accurate to allow for confirmation that this approach could be used as a general predictor of relative elution on GC×GC; however, this application may have been too subtle a problem to reduce mathematically. Studies of essential oil analysis yield two main observations. First, a column set that gives an enhanced separation of oxygenated components (e.g., oxygenated mono- and sesquiterpenes) will be useful to "pull apart" these regions and provide resolution of the complex components. A BPX5–BP20 set has been used for this task. However, for the different hydrocarbon components (saturated and unsaturated terpenes) it may be that this column set is not the best. This gives an extra complexity to the determination of the instrumental requirements for optimized separation. For chiral analysis, we have used both the chiral column in the first dimension and second dimension to compare the performance of analysis for lavender. Chiral components are displayed as pairs of peaks in either the first dimension or second dimension, respectively. As to which is the preferred presentation, that will likely depend on interferences in the sample.

Seeley (16) used two different phase combinations to study a range of synthetic mixtures choosing two columns that gave enhanced identification power for all components. The column set was comprised of a 10-m-long thick-film (1.4 µm) primary column of DB624 phase with 5-m-long secondary columns of 0.25-µm-film-thickness DB-Wax and 0.50-µm-film-thickness DB-210 phase. All columns were of the same inner diameter (0.25 mm).

Column dimensions. The GC×GC result can only be achieved if the analysis on column 2 is performed "fast". Thus, a complete elution on column 2 will be required in a few seconds. This puts certain demands on column 2, thus it will usually be a short column of narrower inner diameter and with a thin film thickness. It should be noted that generally column 1 is a conventional capillary column, but it can also equally be a shorter column than traditionally used. Therefore, as the technique continues to evolve, new concepts in the implementation of coupled column geometries will develop. The narrow-bore column will have a much faster average linear carrier flow velocity (e.g., going from a 0.25-mm-i.d. to a 0.1-mm-i.d. column will result in a carrier flow increase of approximately 6-fold). This may have implications on the efficiency of column 2, thus column 1 could be operated at a much lower flow than normal to allow column 2 to exhibit its best performance. It is not a strict requirement that column 2 should be a narrower-bore capillary column. It should be appreciated that variation in column flows through column 1 will deliver solute to column 2 at different temperatures when a temperature program operation is used, thus this affects the retention on column 2. Because the relative separation of components will also be a function of temperature, the interplay of experimental conditions in terms of optimization will be rather complex. As a starting position, a 1- to 1.5-m column of 0.1-mm i.d. might be used in the second dimension, but some of our work has also used columns as short as 30 cm. Again, this depends on the k values and carrier flow in this dimension. Column film thickness may be as low as 0.05–0.1 µm, and this has an impact on column activity if very polar or acidic/basic components are to be analyzed.

The differential flow technique differs from those previously mentioned in as much as a high flow is required through column 2, thus the use of narrow columns has not been suggested and

similar inner dimensions for columns 1 and 2 have been employed.

Detector considerations

Flame ionization and electron capture. Fast data acquisition is critical for fast GC peaks, thus with peaks having a 150-ms base width and smaller (peaks as narrow as a 50-ms base width have been reported) then 50–100 Hz data frequency is needed. A 50-Hz detector acquisition for a 50-ms base width peak will give maybe five measurements over the peak (it should be noted that the peak is wider than the 4σ width given by the conventional base width measure), which will be inadequate to draw an accurate peak shape. Ten points would be preferable, thus 100 Hz data acquisition is preferred in this case.

Not surprisingly, flame ionization detection (FID) has been the detector of choice in most GC×GC works to date. It was the first of the regular GC detectors available for fast analysis, and today 100–200 Hz operation is available in newer GCs. Some early users of GC×GC modified their slow detectors to be compatible with fast peaks. Faster data acquisition, however, also means greater noise levels (noise increases as the square root of the data rate increases), because the slower rate acts as a buffer to the natural electronic noise fluctuations of the transducer. This affects the sensitivity enhancements that GC×GC can achieve (as will be discussed).

Other ionization detectors will be generally suited for fast operation if the same electronic data-handling circuitry as the FID is used. The other major requirement is that the detector transducer responds in a reliable fashion to the rapid flux variation in the detector cell. Thus, the time constant of response must be commensurate with the peak mass flux profile. The electron capture detector also is now available as a fast data rate device, and the thermionic detector should be likewise relevant to GC×GC use. Just as packed column detectors underwent a technical improvement when capillary columns were developed, regular capillary detectors must also be redesigned for very fast GC. Microcell designs with smaller internal volumes will be required to preserve the narrow time profiles of the GC peaks. Few applications are presently available on those other than the FID, thus further developments in the use of different detectors are awaiting.

Mass spectrometry. There are two aspects of interest with respect to mass spectrometry (MS) when applied to GC×GC. First, many laboratories routinely use GC–MS to provide some measure of identification for their GC analyses. Thus, there is an expectation that MS should be available for GC analysis. The second aspect is that given the considerable separation power that GC×GC has demonstrated for complex samples, it is important that the separated peaks be unambiguously assigned to specific molecular species, thus MS will validate the claims of the high-resolution nature of GC×GC and provide valuable confirmation of its superior molecular discrimination.

The same considerations of data-acquisition speed will equally apply to MS. Thus, the MS must present data at the rate of one mass spectrum (or one scan) every 0.02 s or better. This acquisition data rate is beyond the rate that standard scanning quadrupole MSs can presently achieve, thus conventional MS is unsuitable for GC×GC analysis. However, one report indicated that the GC×GC analysis could be slowed down to allow one reasonable scan across a peak and thus confirm peak identity (21). Such an approach is tedious and unlikely to be very practical, but it was a useful study that pointed out the demands that GC×GC places on the MS detection step. Time-of-flight MS (TOFMS) technology permits data acquisition at thousands of spectra per second; these data may then be bunched to allow for presentation at up to 100 spectra/s. This is sufficiently fast for GC×GC applications. Presently, only a handful of applications have used TOFMS for GC×GC analysis, such as for petroleum products and essential oils (22,23). These have clearly shown that TOFMS does offer to GC×GC the necessary quality of spectra to permit identification and library-searching capabilities to support the interpretation of the complex 2D separation maps of GC×GC. One drawback is that the TOFMS suppliers do not offer data systems that support GC×GC data presentation formats, thus data manipulation is still very much a manual operation. Data files are also very large (hundreds of megabytes).

There is, however, one fundamental advantage that GC×GC offers. In many analyses of overlapping compounds, GC–MS is the only way to obtain a unique quantitative analysis of the sample. Thus, GC–MS is necessary for the apportionment of the proper amounts of each compound in the unresolved chromatogram. With GC×GC the components are now largely completely

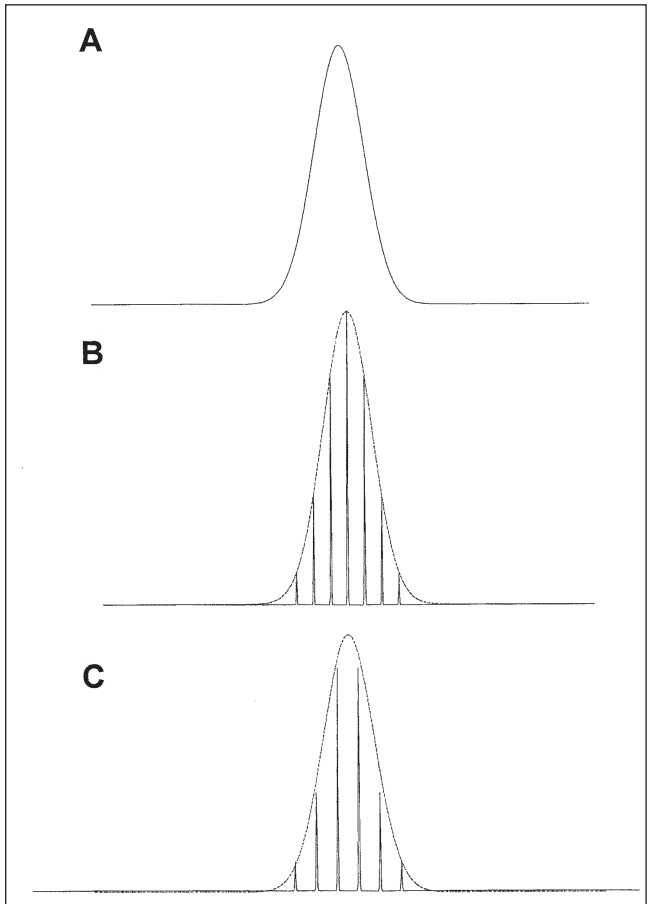

Figure 2. A normal nonmodulated GC peak (A), in-phase modulated GC peak pulses in GC×GC (B), and 180° out-of-phase modulated GC peak pulses in

resolved (provided that the correct column set is used) and TOFMS is not required for the quantitative analysis of all samples, apart from the initial decision of locating and identifying compounds within the 2D map. Once these have been assigned, the GC×GC analysis can be used with confidence for all analyses of the same sample type, without requiring TOFMS.

The current interest in both GC×GC and TOFMS should produce a rapid expansion in availability and use of GC×GC–TOFMS facilities in the near future.

Modulation phase and frequency

Effect of modulation phase and frequency (conceptual framework)

Murphy et al. (24) considered the effect of sampling rate on resolution in a comprehensive two-dimensional liquid chromatography (LC×LC) experiment. Included in the study were comments on the effect that sampling phase had on resolution. Results were presented only as 2D plots, thus the effect that the phase had on the sequence of pulses in the second dimension was not clear. The nature of the study and chromatographic modes employed did not lead to the very high resolution and sensitivity attainable in GC×GC, because zone compression effects usually accompanying the GC×GC modulation process were not so readily achieved in LC×LC. Therefore, it was instructive in this study to investigate the same concepts in the GC arena. They did, however, conclude that the primary dimension peak should be sampled at least three (and in some cases four) times into the second dimension if the resolution is not to be degraded. Also, it has been repeated in a number of literature reports that the modulation of the chromatographic signal eluting from the first dimension in GC×GC should be of a frequency that leads to "several" slices of each peak being delivered to the second column (25). Thus, if a peak is 20 s wide at its extremities (it should be noted that this is a broader definition than the formal base width of a peak), then use of a modulation duration of 4–5 s might be indicated. Narrower peaks will therefore either require faster modulation or have fewer modulation events. There has been little discussion in the literature as to the implication of these choices. In addition, not only is the number of modulations across each peak of concern, but also is the relative "position" of the modulation over the chromatographic signal. Both of these parameters will have an effect on the presentation of the pulsed peak profiles generated on the second column in terms of the number of pulses and also the shape of the pulsed peak envelope.

In the work described in this study, the relative position of the modulation events with respect to the chromatographic band is referred to as the phase of the modulation. Figure 2 illustrates two modulated peak profiles for modulation phases that are maximally out-of-phase. Figure 2A is the nonmodulated peak produced at the detector. Figure 2B and 2C are pulses that should essentially have the same envelope shape as the peak outline in Figure 2A. Although these three diagrams are drawn exactly aligned, the cryogenic trapping process will delay the peaks' passage (by up to the duration of the trapping event time) through the trap, and thus the arrival time of the peak at the detector will not exactly match that of the nonmodulated case. Therefore, the lower traces should be slightly offset to longer retention times (t_Rs).

Figure 2B is a trace that gives a symmetric pulse sequence with a single maximum peak. This case will hence be referred to as the in-phase case. Figure 2C is still symmetric but has two (equal) maxima; this is the 180° out-of-phase case. These will give the tallest and smallest maximum responses for the modulated peak pulses, respectively. Any intermediate modulation phase will generate an asymmetrical profile, and the tallest peak will be between the two limiting response maximum conditions. Each set of pulsed peaks will have the same total peak areas (equal to that of the peak in Figure 2A). The absolute peak heights of Figures 2B and 2C compared with Figure 2A will depend on the frequency of modulation and will both be considerably taller than the peak in Figure 2A. Thus, if a modulation zone compression event is symmetric about the peak maximum (mean) (i.e., it includes the peak mean and an equal amount of band at either side of the mean) then it will be called in-phase modulation.

The modulation process can be stepwise varied in its phase from being in-phase through to the 180° out-of-phase position, in which one compressed zone collects the part of the band immediately prior to the peak mean position and the next collects the part immediately after the peak mean. It follows then that between 180° and 360° the modulation events shift away from this out-of-phase position to eventually again be in-phase (at 360°). Because each of these phase settings effectively pulses different amounts of solute over the total chromatographic peak, the series of pulsed peaks for each phase will produce a different display of pulsed peaks (both in position and amplitude). It has been long recognized that the peak maximum given in GC×GC depends on which part of the peak is collected in the largest flux of material. Recently, Lee et al. (26) produced a model for this variation in amplitude enhancement that can be achieved with an exponential relationship between the modulated secondary column peak width and the amplitude enhancement proposed (26). The model confirmed the well-recognized effect that collection duration will have on the peak height increase in the GC×GC experiment. However, an experiment that demonstrates this quantitatively during a chromatography analysis was not described. In this study such an experiment will be illustrated. Described will be how the experiment may be conducted, and it was explored how the variables may be adjusted. Peak maxima and the t_R value changes that are obtained from different modulation phases were compared, and results illustrate that the pulsed peaks obey the cumulative distribution function for a Gaussian peak. Although this should be expected, it is useful to show this effect experimentally. In this case, the pulse period used to modulate the peak may be represented in terms of the standard deviation (SD) of the peak width. Finally, an example of a multicomponent sample consisting of semivolatile aromatics was used to demonstrate how the modulation duration affects the resolution in a 2D presentation of GC×GC data.

The relationship between modulation timing events and peak elution time is normally "random", thus there is usually no discussion of the modulation phase and subsequent peak pulse profiles obtained from the GC×GC experiment. Therefore, the pulses of peaks seen in GC×GC may be anywhere from in-phase to 180° out-of-phase, and the appearance of different phases for pulsed peaks should be recognized and accepted. By sequentially altering the modulation phase in successive chromatographic analyses

with a presentation of the series of pulsed peak profiles generated that demonstrate the effect of the relative modulation phase, a series of phases from in-phase through to 180° out-of-phase cases may be defined. The two limiting cases (in-phase and 180° out-of-phase) produce symmetric peak pulse profiles. The t_R of the maximum pulsed peak varies according to the modulation phase, and the peak height enhancement depends both on the frequency and modulation phase employed. Estimation of the real peak t_R (peak mean) of a modulated peak can be derived from the peak pulse areas. The contour plot of a peak that is generated in two dimensions also depends on the frequency and phase of modulation. The slowest modulation period used in this study gave up to a 30% difference in contour width (depending on the manner in which the peak was modulated), and this had ramifications on the apparent resolution seen in the contour plot of a complex sample.

This study that was designed to illustrate these effects will be outlined in some detail and has not been previously reported in the literature.

Experimental

Equipment

A Model 6890 GC (Agilent Technologies, Burwood, Australia) fitted with an FID operated at a data-acquisition rate of 100 Hz, a split/splitless injector operated in 1:10 split mode, and a 7683 Series (Agilent Technologies) automatic liquid sampler was used throughout. Hydrogen was employed as the carrier gas and operated in the constant flow mode. ChemStation event control (Agilent) was used to instruct the modulation control system to commence modulation at a precise time, and the ChemStation data system (Agilent) was used to record the detector output. It should be noted that in this study, it was important that the modulator timing be very precise (i.e., the modulation events be controllable to better than 0.1 s, for example) and in particular that the commencement time of the modulator be accurate. In the system used in this study, the run-to-run reproducibility exceeded that required, thus allowing the effect of the modulation phase to be studied.

The cryogenic modulator employed for the GC×GC experiment was the LMCS Everest Model (Chromatography Concepts, Doncaster, Australia), which was retro-fitted to the 6890 GC. CO_2 maintained the temperature of the modulation trap to at least 100°C below the prevailing oven temperature. The operation and demonstration of the principles of this system can be obtained elsewhere (27,28).

Column sets and experimental procedure

A dual-column arrangement comprised of a primary column of 25-m × 0.22-mm i.d. with a 1.0-µm film thickness (BPX5-coated column, 5% phenyl-dimethyl siloxane phase, nonpolar) directly connected to a short second column of 1.2-m × 0.1-mm i.d. with a 0.1-µm film thickness (BPX50-coated column, 50% phenyl-equivalent polysilphenylene phase, polar) was used for all studies. Both columns used were manufactured by SGE International (Ringwood, Australia).

The cryogenic trapping system was operated under selected modulation timing periods (or durations) of 2, 3, 4, 6, 8, or 9.9 s (as indicated in the respective phases of this study) and a hold time of 0.5 s in the release position. For studies using linalyl acetate, the modulator start time was at least 1 min prior to the expected solute t_R (i.e., approximately 16 min). In some studies the start time was sequentially incremented by 0.01 min in order to alter the modulation phase of the cryotrap with respect to the peak elution. By appropriate calculation it was possible to estimate a start time that will give an in-phase modulation, and from this start time the modulation phase was then varied in 0.01-min intervals until the cycle was completed (i.e., through 180° out-of-phase to 360° in-phase). The GC oven was operated under a temperature program rate of 60°C (held for 1 min) heated to 120°C at 20°C/min, then to 150°C at 2°C/min, and finally to 180°C at 20°C/min. This temperature program was used to give a suitable peak width such that a range of modulation frequencies could be used to study the effect of this variable (i.e., giving a number of pulsed peaks for the intermediate frequency chosen) and permit a number of modulation start times incremented by 0.01 min to be used.

Modulation timing periods of 2, 3, 4, 6, 8, and 9.9 s were used for the semivolatile aromatics. The modulation start time was kept constant while the modulation timing periods were varied. The semivolatile aromatic mixture was analyzed using a temperature program of 40°C (held for 1 min) heated to 150°C at 20°C/min and then to 230°C at 2°C/min. A split ratio of 40:1 was employed.

Samples

Linalyl acetate was provided by Australian Botanical Products (Hallam, Australia), and the semivolatile aromatic sample was from

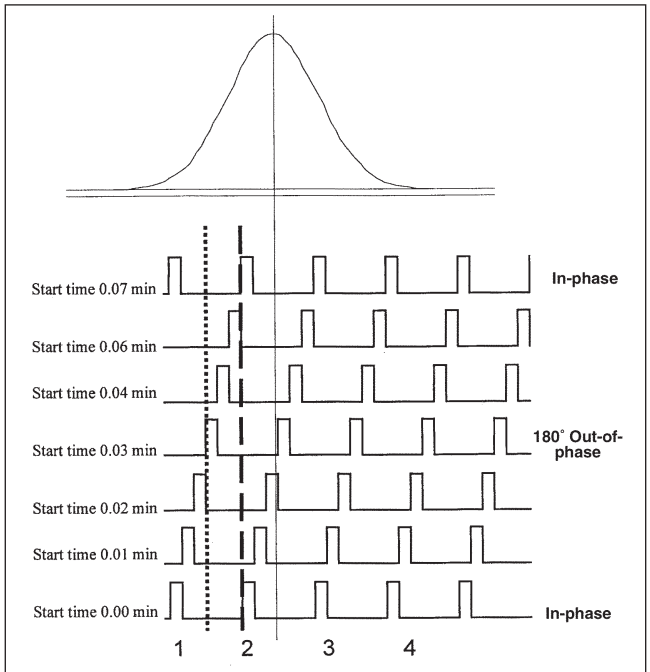

Figure 3. Correlation of phase of modulation and peak elution. A delay of 0.03 min results in a 180° out-of-phase modulation case with the 0.03-min delay exactly midway between pulses 1 and 2 in the original modulation (dotted line), and a 0.06-min delay gives a result that is in-phase with the original modulation (dashed line). The vertical line shows that the central zone of the peak is exactly captured in the third modulation and thus this will give an in-phase result equivalent to Figure 2B.

Ultra Scientific (Kingston, RI) (part number SVM-124-1). Linalyl acetate was diluted with hexane in order to prevent overloading of the peaks when the GC×GC experiment is conducted. The same linalyl acetate solution was used throughout this study apart from that used for experiments for the reproducibility of retentions and the studies of modulation timing periods of 3 and 4 s.

Results and Discussion

Correlation of modulation phase with peak elution

In order to demonstrate how the two different results (Figure 2B and 2C) and the intermediate pulse profiles were generated, Figure 3 presents a pulse train that shows the positions of the cryomodulator and the relative event times for the commencement of the modulation of the cryotrap that may be used. The vertical rectangular pulses represent when the trap moves to the elute position. A hold time of 0.5 s was imposed, and the return movement to the home trapping position occurred when the rectangular pulse returned to the baseline. Figure 3 shows that in successive GC analyses, the trap was delayed in the modulation start time by 0.01 min. With a delay of 0.03 min, the peak pulses were still out-of-phase (by 180°) with the original sequence. In order to reach a modulation sequence exactly in-phase with that used initially, the delay would need to be 0.06 min = 3.6 s, thus the modulator was operated at a pulse duration of 3.6 s for this example.

If a migrating peak entered the cryomodulator such that its central zone was fully collected in one trapping event (i.e., the trap event was symmetrical about the peak maximum), then a symmetric peak profile of the type in Figure 2B was obtained. It should be noted that there is no control over this situation in a normal GC analysis, and among the pulsed GC×GC peaks it may be that none of them give an exact symmetrical set of peak pulses.

In Figure 3, the modulation timing can be adjusted to give a range of phases between 0° and 180° (i.e., fully out-of-phase) and up to 360° (in-phase with 0°). In order to present sufficient comparative profiles over a full 360° phase change, a variation in the commencement of successive GC experiments of 0.01 min was chosen. Thus, for a 3.6-s modulation period (0.06 min = 360°), there were six successive GC analyses before the modulator repeated the original pulsing phase pattern (60° for successive experiments).

Table I. Reproducibility of Peak Retentions in Normal GC Mode

Run no.	t_R (min)	Peak area (pA•s)	Peak height (pA)
1	6.427	73.781	23.858
2	6.431	74.164	24.214
3	6.432	73.784	24.260
4	6.432	75.190	24.231
5	6.433	74.902	24.204
6	6.432	74.880	24.290
7	6.431	74.540	23.863
8	6.432	74.538	24.092
9	6.433	75.164	24.031
10	6.432	75.086	24.248
11	6.433	75.447	24.496
Average*	6.432	74.680	24.162
SD*	0.002	0.570	0.189
%RSD*	0.026	0.764	0.783
Average†	6.432	74.769	24.193
SD†	0.001	0.513	0.169
%RSD†	0.011	0.686	0.697

* All data.
† Rejecting Run #1 data.

Reproducibility of retentions

In order to appropriately study the effect of the modulation phase experimentally, it is a requirement that the run-to-run reproducibility of peak retentions is better than the time variation of the modulation experiments (e.g., 0.01 min above). This will ensure that the comparison of peak profiles in successive experiments will be meaningful. The 0.01-min interval in the modulation start times was 0.6 s. The peak retention reproducibility should be much better (i.e., smaller) than this. Table I lists data for peak retention in 11 repeat nonmodulated experiment analyses. The SD of peak t_R was 0.002 min (or 0.12 s), thus this was 5 times smaller than the time variation of the modulation phase and should be suitable for the study as proposed. The first entry in Table I (6.427 min) may be rejected as an outlier, which gives much better t_R reproducibility. Peak areas and heights each had a relative SD (RSD) of 0.8%.

Table II. Reproducibility of Peak Retentions in the GC×GC Mode*

Chromatogram from Figure 3	t_R for peak pulse no. (min)				Δt_R values between peak pulses (min)		
	1	2	3	4	2-1	3-2	4-3
A	17.052	17.102	17.151	17.201	0.050	0.049	0.05
B	17.052	17.102	17.151	17.201	0.050	0.049	0.05
C	17.052	17.103	17.153	17.201	0.051	0.05	0.049
D	17.052	17.102	17.152	17.201	0.050	0.05	0.049
E	17.052	17.103	17.153	17.201	0.051	0.05	0.048
Average	17.052	17.1024	17.152	17.201	0.0504	0.0496	0.0492
SD	2.4×10^{-7}	0.00055	0.0010	3.4×10^{-7}	0.00055	0.00055	0.00084
%RSD	1.4×10^{-6}	3.2×10^{-3}	5.8×10^{-3}	2.0×10^{-6}	1.1	1.1	1.7

* A 3-s modulation duration was used giving Δt_R values close to 0.050 min for successive pulses.

The modulator reproducibility was then checked by successive injections of the same sample. A pulse duration of 3 s (0.05 min) was used. Table II lists these data. The SD and RSD values for most of the retentions were so small as to be negligible (e.g., RSD of 0.006% or less). The improved peak time reproducibility compared with that in Table I arose from the very precise release time of the modulator and the short column length, thus a small t_R interval on this section of the column between the modulator and detector. Carrier gas flow precision will also be

Table III. Reproducibility of Absolute Peak Pulse Areas for a 3-s Modulation with the Largest Four Pulsed Peaks Reported

Chromatogram from Figure 4	Peak areas for peak no. 1	2	3	4	Total peak area
A	20.45	113.78	122.04	25.04	281.32
B	10.22	83.74	141.57	43.7	279.24
C	8.79	77.71	143.54	49.29	279.33
D	6.66	69.52	142.27	53.59	272.03
E	7.7	73.34	142.85	52.26	276.15
Average*	10.76	83.62	138.45	44.78	277.61
SD*	5.57	17.67	9.20	11.67	3.63
%RSD*	51.78	21.13	6.65	26.06	1.31
Average†	8.34	76.08	142.56	49.71	276.69
SD†	1.52	6.11	0.84	4.39	3.44
%RSD†	18.27	8.03	0.59	8.83	1.24

* All data.
† Rejecting data of Figure 4A.

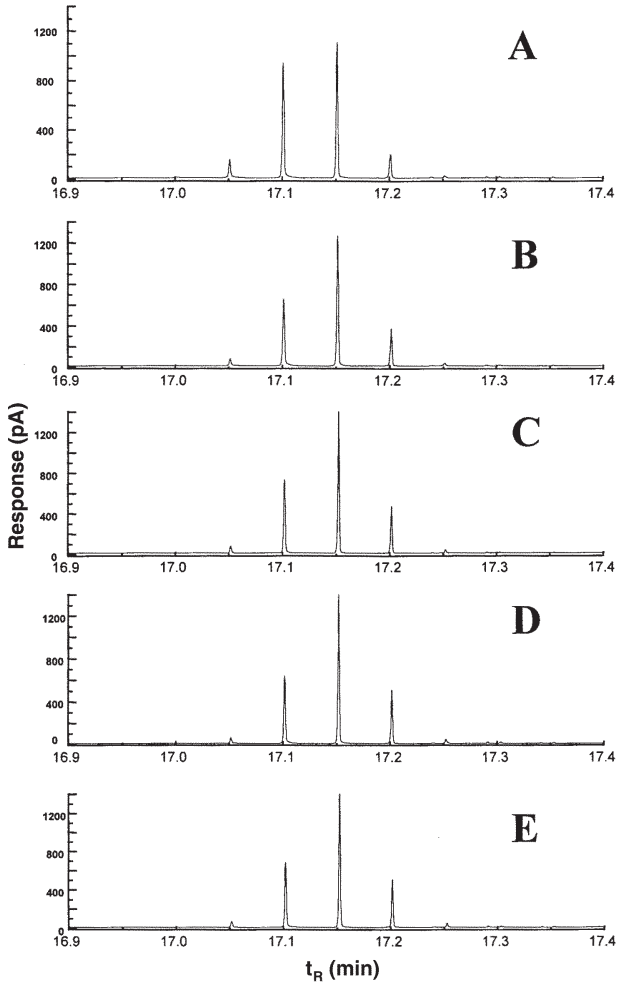

Figure 4. Reproducibility of peak pulses generated using a 3-s modulation duration for linalyl acetate (conditions found in the Experimental section) in successive chromatographic analyses. The chromatogram in A is an anomalous result (as seen in Table III). The profiles for the chromatograms in B through E are very reproducible.

critical. This appeared to be excellent.

Although t_R values are very precise, the peak areas and heights of the pulsed peak profile are less precise. Table III reports these data. The first analysis may be rejected, and the resultant improved reproducibility can be seen in Table III. Considering these latter data, it is apparent that the profile was well-reproduced. It was presumed that the small variations in Table III were a result of slight peak retention differences when the peak enters the cryotrap, which means that the mass flux of solute into the cryotrap in a given peak pulsing period varied slightly. Total peak area reproducibility was good. The first entry again appeared to be an outlier, although there did not seem to be a reason for this. Deleting this row of data gives improved reproducibility (as shown in Table III). Figure 4 illustrates the five GC traces for this data, and the anomalous first run is apparent. It can be concluded that the GC and modulator performance were suitable for the proposed study.

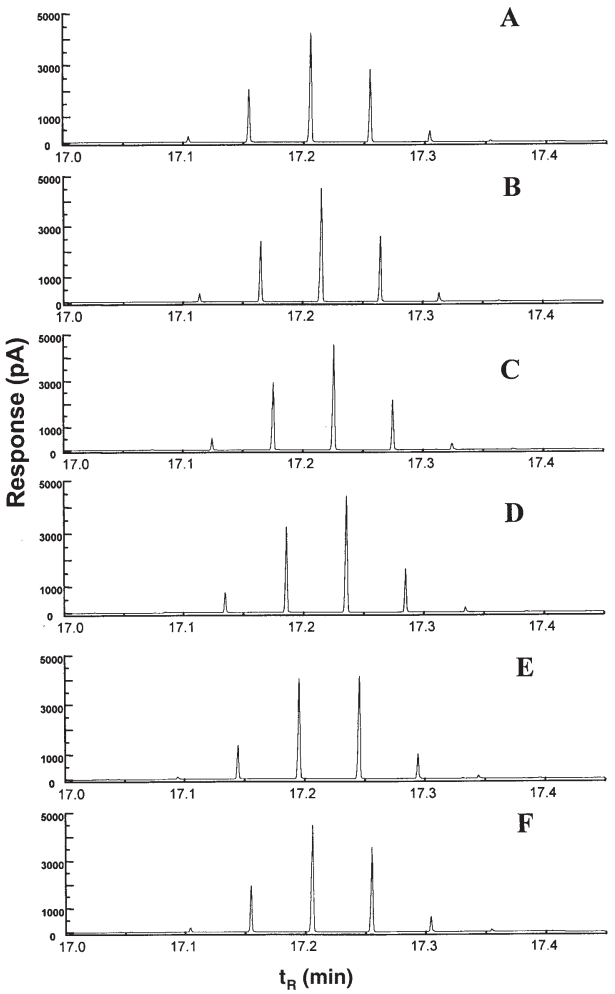

Figure 5. Variation in the phase of modulation for a 3-s modulation duration (conditions are the same as in Figure 4). The modulation phase was altered by successively delaying the start time by 0.01 min from A to F, with an initial start time of 16.00 min. A and F approximate the same modulation phase, thus produce almost equivalent results. The time shift in the maximum peak can be readily seen in this series of analyses. Table IV presents the pulsed peak times and areas for the chromatograms in this figure.

Variation in modulation commencement time

By varying the start time of the modulator for a series of GC analyses and with the peak t_R unchanging, it is possible to have a controlled variation in the phase of the pulsing of zones of the migrating peak. Figure 5 illustrates this behavior. Because a modulation duration of 3 s was used and the modulation start time was incremented in steps of 0.01 min, after 5 increments the same modulation phase was repeated. Thus, it can be seen that Figure 5A should be reproduced in Figure 5F. This was approximately the case. It should be noted that the profile pattern of peaks moved to the right in steps of 0.01 min, and as this shift occurred with the input peak position to the cryomodulator unchanged, there started to appear an earlier peak while the latest peak appeared to diminish. The largest peak in Figure 5A at 46.7% of the total area progressively decreased to 32.7% in Figure 5F (as the zone that was compressed in the cryotrapping process progressively decreased because this modulation event moved towards the trailing end of the peak) when it had the same time as the fourth peak of Figure 5A with an area percentage value of 27.8%. The second peak in Figure 5A steadily increased from 19.3% to 44.0% in Figure 5F when it had the same time as the largest peak in Figure 5A (which had an area percentage value of 46.7%). Table IV lists the data for the respective peaks in these traces. The time of peak 1 was 17.104 min for Figure 5A and increased sequentially by 0.010 min up to 17.135 min for Figure 5D. In Figure 5E, a new first peak appeared because of the phase shift of the modulation (thus it had a time of 17.094), and finally in Figure 5F the modulation was 360° out-of-phase from that of Figure 5A, which means it became in-phase (thus the first peak again had a time of 17.104 min). The tallest peak in the traces varied from an area percentage of 47.7% (Figure 5B) to 39.9% (Figure 5E), which was a change of approximately 16%. This occurred as the peak profile changed from a symmetric distribution (represented by Figure 2B) to a symmetric distribution (represented by Figure 2C). These two experiments varied by 0.03 min, which was close to the 180° out-of-phase value of 0.025 min (it should be noted that there was no pair of figures that had an exact 180° difference because the modulation time was varied by 0.01 min in each step). The total peak areas varied from 1038 to 1185 pA•s, but this generally will reflect sample delivery efficiency and should not alter the peak area percentage values.

Figure 6 and Table V report the same study as described previously, except with a modulation duration of 6 s (double that used previously). The modulation start time was again varied by 0.01 min. The figures presented were every second in the series, thus they were 0.02 min apart. Figure 6C approximates one of the symmetric profiles and Figure 6F approximates the other. It should be noted that the largest peak in Figure 6F had an area percentage of 81%, whereas it was 49.5% in Figure 6C. This equates to an area difference between maximum peaks of approximately 39%. The large variability was of course a result of the large amount of peak that was zone compressed in the case of Figure 6F (Figure 6C was designated for a modulation event almost exactly at the peak maximum), and this effectively shared the bulk of the peak equally between the two-zone compression events. The larger the pulse period, the greater is the anticipated variation in the peak maxima for the in-phase and out-of-phase cases (as can be seen by comparing Tables IV and V).

Modulation frequency variation correlations

It is commonly accepted that approximately 4 or 5 pulsing events are preferred for a solute in GC×GC; however, the actual number pertaining to a given analysis is often not given, nor has the choice of frequency been reported in terms of how the data compare. The greater the number of modulations over a peak, the less is the sensitivity enhancement that is realized in the GC×GC experiment over normal GC. Also, from the previous section, the presentation of peak pulses will also vary considerably for different modulation periods employed. It is beneficial to investigate the variation of frequency over the peak elution and observe how this alters the peak contours in the 2D plots that are used for data presentation in GC×GC.

If a set modulation start time is used for a series of different modulation durations, then the pulsed peak profile will also vary according to the phase of modulation across the peak. Thus, one modulation setting may give a symmetric pulsed peak profile and another might be significantly asymmetric. If the experiment is conducted using a range of different start times for each of the modulation frequencies to be used, then it will be possible to select from the whole data set a series of pulsed profiles of similar modulation phase (e.g., in which all give symmetric distributions).

Both of these cases will be instructive in the interpretation of the results. It should be noted that it would be possible to compute which frequencies should give which pulsed peak profiles

Table IV. t_Rs, Peak Relative Areas, and Total Peak Area for a Series of Phase Increment Analyses in 0.01-min Steps Using a 3-s Modulation Duration*

	Figure 5A		Figure 5B		Figure 5C		Figure 5D		Figure 5E		Figure 5F	
	Time (min)	%Area	Time (min)	%Area	Time (min)	%Area	Time (min)	%Area	Time (min)	%Area	Time (min)	%Area
Peak 1	17.104	2.2	17.114	3.0	17.125	4.4	17.135	6.4	17.094	0.8	17.104	1.6
Peak 2	17.155	19.3	17.165	22.1	17.176	26.8	17.186	31.1	17.145	11.1	17.155	15.8
Peak 3	17.206	46.7	17.216	47.7	17.226	47.7	17.236	46.4	17.196	38.9	17.206	44.0
Peak 4	17.255	27.8	17.265	23.9	17.275	18.6	17.285	14.4	17.246	39.9	17.256	32.6
Peak 5	17.304	4.1	17.314	3.3	17.324	2.4	17.335	1.8	17.294	8.2	17.304	5.2
Peak 6									17.345	1.1	17.355	0.8
Total peak area		**1039**		**1095**		**1111**		**1101**		**1162**		**1186**

* Two analyses gave six peak pulses.

by estimation of the modulation phase during peak elution. Figure 7 presents data for a series of modulation frequencies (2-, 3-, 4-, 6-, and 9.9-s period) for the same start time (16.03 min). Figure 7A (2 s duration) gives approximately 7 pulses across the peak. The maximum pulsed peak was at approximately 17.14 min. A 4-s pulse modulation gave only 3 peak pulses (the maximum being at approximately 17.12 min). Three pulses were also seen for a 6-s period (maximum pulse at 17.175 min) and the 9.9-s modulation (2 peaks) (maximum pulse at 17.225 min). The maximum peak among the pulsed sets clearly shifted in its t_R value, and the latest possible maximum peak elution was where the slowest modulation (9.9 s in this case) commenced in collecting the migrating solute just prior to the peak maximum flux entering the trapping zone. In this case the t_R value of the latest possible peak was equal to approximately the sum of the time that the cryotrap started collecting the solute plus the t_R on the second column plus the modulation time. Thus, it could potentially be up to 9.9 s longer than that of the peak maximum obtained on the same column set at the same conditions, except that the cryofluid was not turned on.

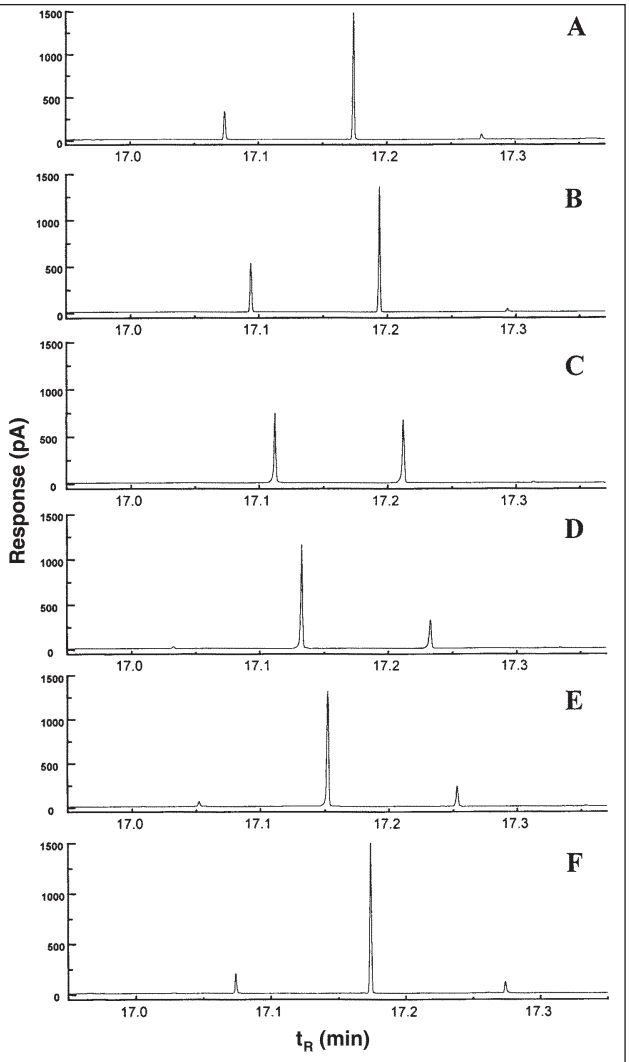

Figure 6. Variation in the phase of modulation for a 6-s modulation duration (conditions are the same as in Figure 4). The number of experiments for a complete 360° cycle was double that for the 3-s duration shown in Figure 5, but only every second result in the series was shown (it should be noted that the pulse peak t_R offset was 0.02 min, compared with 0.01 min in Figure 5). Because the modulation duration was twice that of Figure 4, there were fewer pulses across the peak, but again the result in A is almost reproduced in F, because they had relative phases approximately 360° apart.

The trend in the heights of the maximum peak in each of the chromatograms should be noted. Because the injected quantity may vary, the comparison was made more valid by correcting for this by dividing the recorded peak height by the total area. Table VI shows these values. It should be noted that this interpretation is only a broad trend because it has been shown previously that the peak height of maximum peaks depends on the phase of modulation. The data confirm that the peak height increased with decreased modulation frequency (in this experiment by approximately 230%). A similar result was found for a start time of 16.05 min, and only the comparison of a 3-, 6-, 8-, and 9.9-s pulse duration is shown in Figure 8. The difference shown for 8 and 9.9 s was striking in terms of the t_R of the maximum peak pulse being 17.155 and 17.225 min, respectively (i.e., 0.07 min = 4.2 s different). This arose simply because of the relative phases of the modulation in each case.

It is possible to predict the true peak maximum for these results by having accurate and precise values for the peak responses, because the cumulative peak area for a Gaussian distribution is well-known, thus allowing for the calculation of exactly at which point in the Gaussian peak the modulation event occurs (provided that the peak SD entering the cryotrap is known in time units). Thus, it can be determined by how many units of SD the peak pulse varies from the peak maximum. Then, using this peak's t_R and subtracting or adding the number of SDs times the SD value, the true peak maximum will be estimated. The

Table V. t_R Values, Peak Relative Areas, and Total Peak Area for a Series of Phase Incremented Analyses in 0.02-min Steps Using a 6-s Modulation Duration*

	Figure 6A		Figure 6B		Figure 6C		Figure 6D		Figure 6E		Figure 6F	
	Time (min)	%Area	Time (min)	%Area	Time (min)	%Area	Time (min)	%Area	Time (min)	%Area	Time (min)	%Area
Peak 1	17.074	17.81	17.095	28.12	17.113	49.48	17.033	1.70	17.051	4.14	17.073	10.09
Peak 2	17.175	78.14	17.194	69.21	17.212	48.90	17.132	71.87	17.152	80.61	17.173	81.30
Peak 3	17.274	4.05	17.294	2.67	17.313	1.61	17.233	25.19	17.253	15.25	17.274	8.61
Peak 4							17.334	1.24				
Total peak area		**167.9**		**169.7**		**173.7**		**175.1**		**175.19**		**177.4**

* Most analyses gave three peak pulses (one gave four peak pulses).

result for a 2-s modulation with 6 peak pulses obtained was considered (see Figure 7A). Their percentage areas were found to be 1.84%, 11.52%, 28.04%, 36.42%, 17.7%, and 4.48%. In cumulative areas, these were 0.0184, 0.1336, 0.414, 0.7782, 0.9552, and 1.000, respectively. Standard tables (29) gave SD values for these cumulative areas (with respect to the mean value) of –2.09, –1.11, –0.217, 0.766, and 1.697, respectively (with no derived value for 1.000). This computes to be 0.98, 0.893, 0.983, and 0.931 SD unit differences, respectively, between each of these pulses. Therefore, the reproducible regular modulation process leads to respective peak areas of the pulses in agreement with that predicted for a Gaussian curve, and the real peak maximum time can be derived from the times of these pulses. This is an interesting observation but probably not of too much concern for routine GC×GC analysis. It may, however, aid 2D peak coordinate derivation and presentation if required in a computerized 2D data report.

Presentation of data in 2D contour plots

At a longer modulation duration, some of the solutes showed barely more than one pulsed peak compared with the multiple peaks when a faster modulation was used. Contour plots of these can be used to show how the plotting package constructs the contours for each case. Also, it is instructive to observe the difference that changing the modulator start time causes when generating the 2D contour plots. In this case, the 0.01-min delay in starting the modulator was independent of the data-processing step (which took t = 0 as the commencement of the data stream), and the modulation time was used to construct the data matrix. Shown in Figure 9 is the contour plots for the sequence of peaks

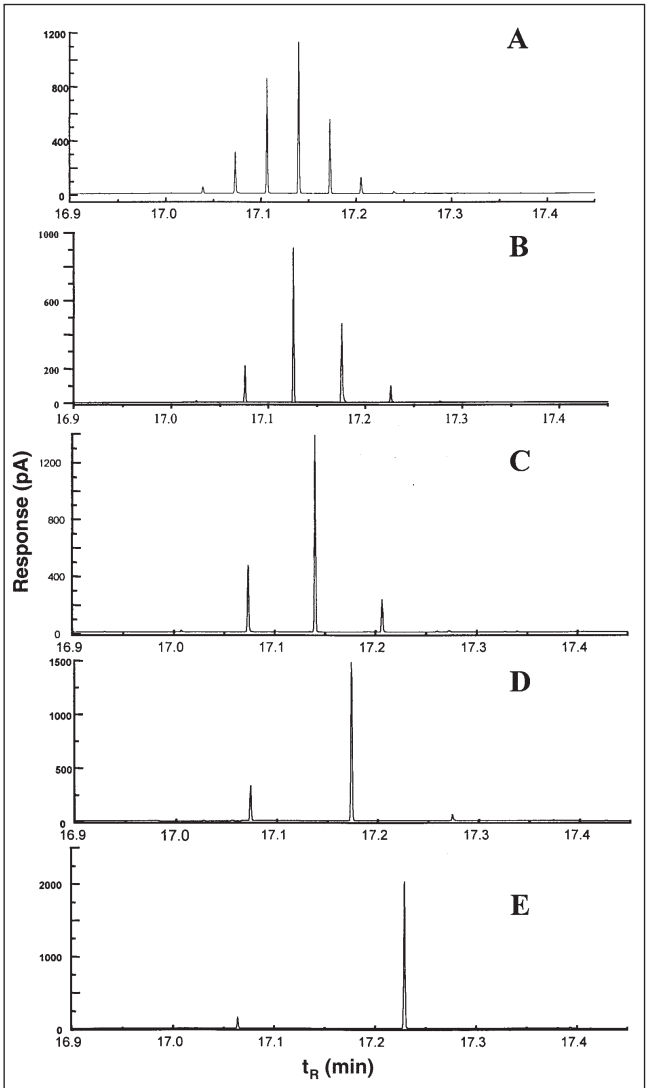

Figure 7. Variation in the frequency of modulation for a constant modulation start time of 16.03 min. The modulation duration was 2, 3, 4, 6, and 9.9 s for A through E, respectively. Other conditions of analysis are the same as in Figure 4.

Table VI. Effect of Modulation Period on the Height of the Maximum Pulsed Peak with a Modulation Start Time of 16.03 min*

Modulation duration (s)	Height of maximum peak (pA)	Total peak area (pA•s)	Normalized height
2	1100	260	4.23
3	900	148	6.08
4	1400	181	7.74
6	1460	168	8.70
9.9	2000	203	9.85

* See Figure 7.

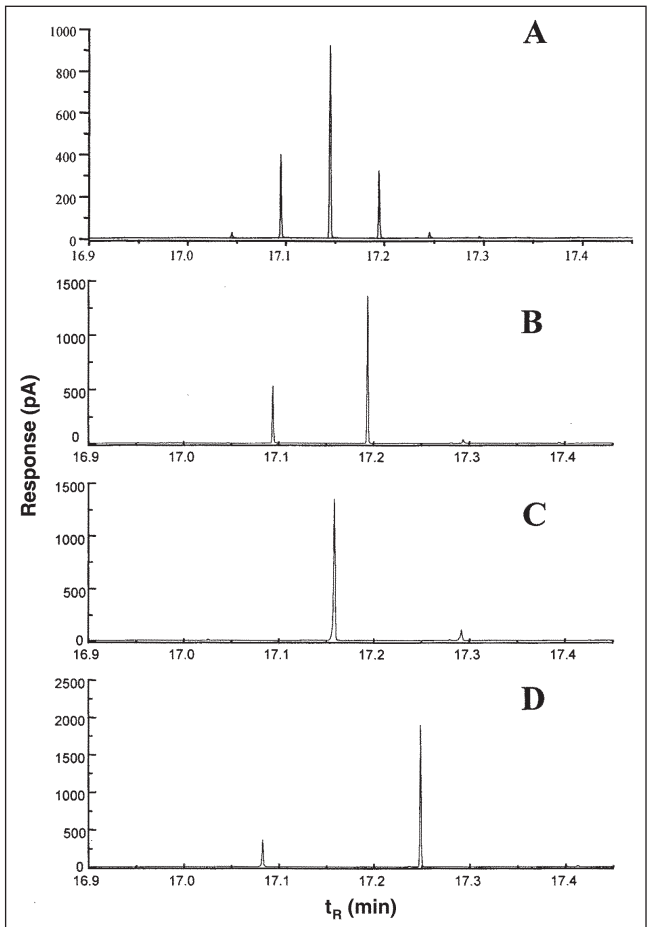

Figure 8. Variation in the frequency of modulation for a constant modulation start time of 16.05 min. The modulation duration was 3, 6, 8, and 9.9 s for A through D, respectively. Other conditions of analysis are the same as in Figure 4.

given in Figure 5. It should be noted that the contours shifted vertically by 0.01 min in the ^2t_R time because they were progressively delayed by 0.01 min in successive chromatograms, and the data conversion was not corrected for this. This has an interesting consequence in general GC×GC 2D plot presentation. If the start time is not precise and the modulation phase varies from run-to-run, the 2D coordinates of peaks will not be well-reproduced. This will potentially make solute identification based on peak position in the 2D space difficult. In this study, excellent positional reproducibility was seen (except for those places in which the start times were deliberately adjusted to alter the phase of modulation).

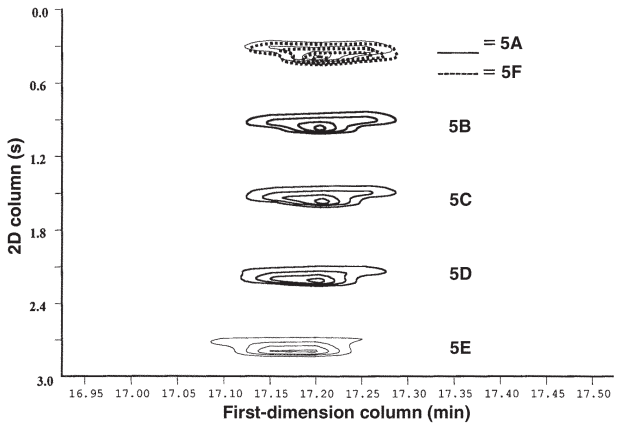

Figure 9. Contour plots for the chromatograms shown in Figures 5A–5F for a 3-s modulation duration. Because these were for different modulation phases achieved by altering the start time of modulation and the data conversion in each instance was not altered to take into account this difference, then the contours were offset successively by 0.01 min (0.6 s) in the second dimension. 5A and 5F are in-phase, thus they plot at precisely the same position.

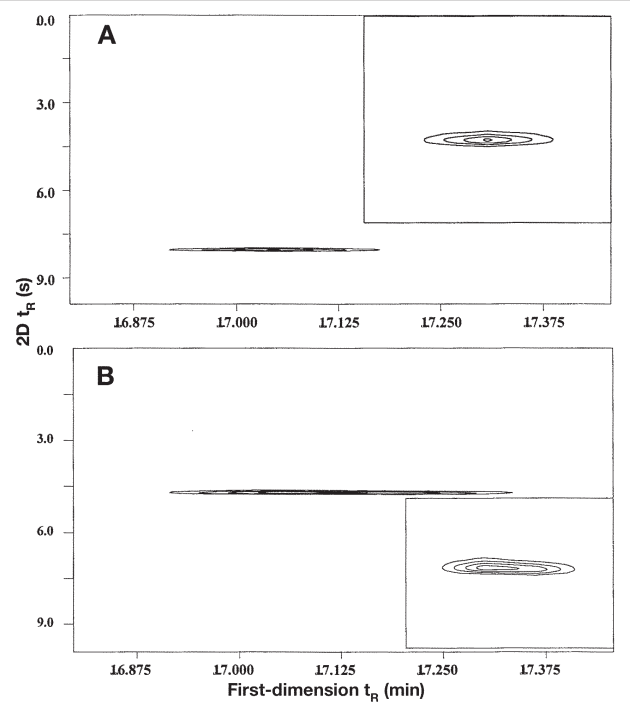

Figure 10. Expanded contour plots for a 9.9-s modulation duration with a different modulation phase. The phase difference was 0.11 min between the two chromatograms (start time for A was 15.98 min and for B was 16.09 min). The pulsed peak profile gave essentially one peak for A and two equal peaks for B.

Peak 5E in Figure 9 was the contour from the pulsed peaks in Figure 5E, and it was plotted at an apparent earlier ^1t_R time compared with the other contours because its peak pulse distribution was more skewed to a lower ^1t_R time. All others were not significantly different, but the excellent correspondence of 5A and 5F should be noted, which were the two in-phase experiments. The contour plots of a 9.9-s modulation rate were almost trivial (Figure 10), because there was at best only two significant peaks. They gave contours of width at 0.26 min and 0.38 min for Figure 10A and Figure 10B, respectively, which corresponded with one predominant peak and two equal peaks in the pulsed trace, respectively. In contrast, the 3-s modulation gave a ^1t_R contour peak plot of width at 0.17 min. We have previously noted the effect of the contour line response in influencing the apparent size of the contour plot (30); in this case a similar contour level was chosen to keep this as consistent as possible. Thus, the effect of the modulation period on contour presentation must be looked upon in a similar way to the effect of overloading and consequent peak broadening in GC×GC analysis (30).

Semivolatile aromatics study

Because in a study such as this with randomly located peak retentions (at least with respect to the modulation phase) a study of variation of phase by altering the start time of modulation appears to be of less utility, it would appear to be relatively easy to implement. However, it has been shown previously that modulation duration strongly influences the apparent contour plot peak magnitudes (widths in the first dimension) of the data when presented in the 2D manner.

Thus, this same multicomponent semivolatile aromatic sample that has been reported elsewhere (31) has been chosen for this study. Because under the conditions chosen the solutes will have a given ^2t_R, when a larger modulation period is selected, the solutes will appear bunched along a narrow elution zone (as seen for Figure 11C at the 9.9-s modulation). In this case, the ^2t_R scale was 9.9-s broad, thus it appears on the 2D space to contract the apparent elution zone. Of course, this range was constant for all modulations, but it only looked wider as the modulation period decreased (i.e., the scale of the ^2t_R axis decreased). From Figure 11C, it can be predicted that the solutes have retentions of approximately 2.5–5.0 s on the second column.

Figure 11A shows a 2-s modulation. From previous considerations, this should give the best (smallest) apparent peak contour plots at a given response level (e.g., 50 pA), and peaks from approximately 60–150 ms width in the second dimension were found. These should also be the most resolved in the first dimension on the plot, having a minimum contour width. By contrast, Figure 11C (9.9 s) shows the effect of longer modulation periods. The peaks marked X (which were well-resolved in Figure 11A) were plotted with a significant merging of their contours. For comparison, Figure 11B was a 3-s period result. Figure 12A is a presentation of an expansion of the peaks marked X (data for the 9.9-s modulation) (Figure 11C), and the pulsed peak result is also shown. Interestingly, even though the pulsed peak result did not clearly show separate pulsed peaks for both components, the con-

tour plot of Figure 12A did show two maxima in the contour. For the 2-s case, the pulsed presentation (Figure 12B) showed two series of pulsed peaks, with an apparent slight resolution for the event in which both compounds were present in the one zone compression step (at approximately 17.69 min). The resolution was quite acceptable in the contour mode. This was in accord with the observation by Murphy et al. (24) that the higher sampling rate gives better resolution. The reason for the double maximum in the first contour peak is not clear. It should also be noted that the two compounds exhibited close to 180° out-of-phase (first component) and in-phase (second component) distributions for their modulated peak pulses, respectively. The peaks marked Y in Figure 11 were well-resolved in the second dimension. Figure 13 shows the two pulsed peak plots for the two components at Y for 2-, 3-, 6-, and 9.9-s modulation periods. The respective peaks were marked 16 and 17 on these diagrams. Expanded contour plots did not need to be presented. All of the examples gave the same retention difference and resolution between components 16 and 17 in the second dimension (as seen in the resolution of 16 and 17 in all of the chromatograms in Figure 13). The difference in the presentation of the pulsed peak chromatograms arising from the choice of frequency was striking.

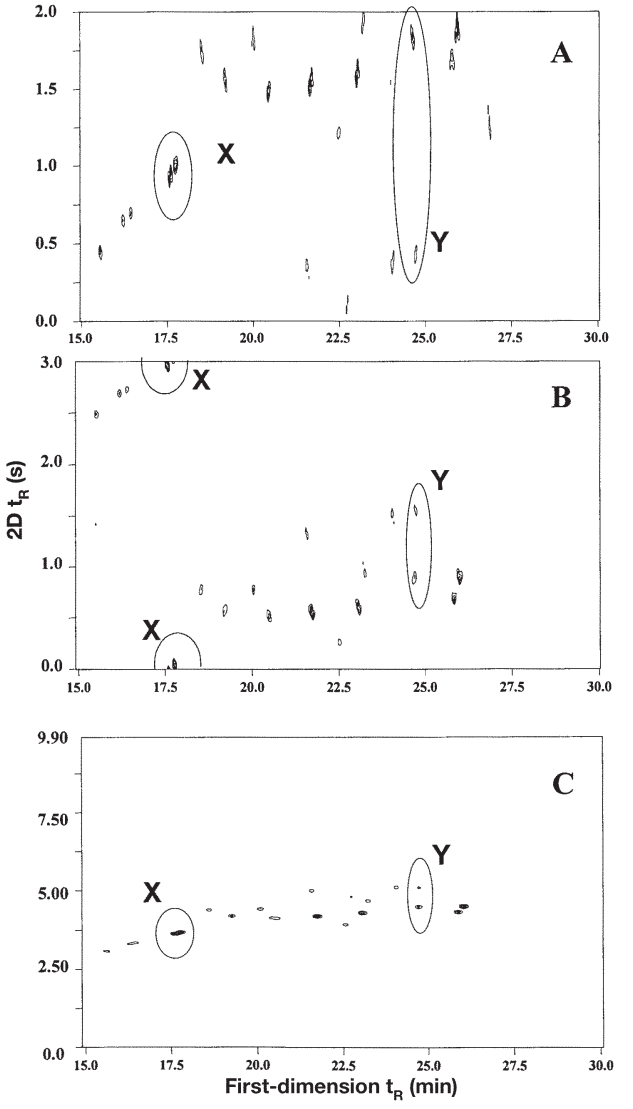

Figure 11. Contour plots for the semivolatile aromatic sample analyzed using different modulation frequencies. A, B, and C correspond with modulation durations of 2, 3, and 9.9 s, respectively. Pairs of peaks with similar first-dimension t_R values are identified by X and Y, with X being poorly resolved on the second column and Y being very well-resolved on the second dimension. For expanded contour and pulsed peak presentations, refer to Figures 12 and 13.

This discussion on the frequency and modulation period is rather complex, although it is not easily reduced to simple description. The terms sound more spectroscopic than chromatographic; however, the different presentation modes for GC×GC should be appreciated and understood by users of this technology as well as the reasons for the generation of different peak pulse patterns. Although the modulation phase affects the resolution, it is not possible to adjust the phase of modulation for each solute in order to artificially select the most appropriate phase (i.e., in-phase modulation) because once the pulse period is set and the start of modulation commences, there is no user intervention to adjust the phase (the modulation phase is a random event for any peak).

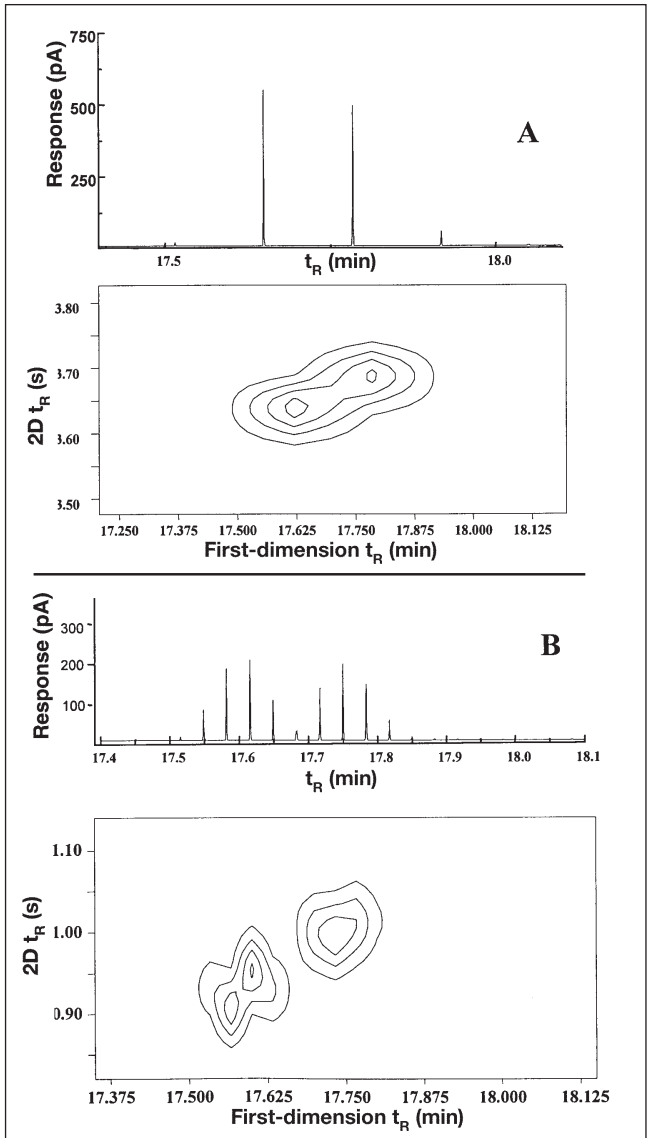

Figure 12. Pulsed peak chromatograms and contour plots for peaks marked X in Figure 11: (A) modulation phase of 9.9 s and (B) modulation phase of 2 s.

Sensitivity enhancement in GC×GC

Any of the modulation methods that yield a zone compression effect (such as the mass flow rate of solute into the detector increases) will be capable of increasing the response sensitivity of the analysis. It should be noted that we have already decided that increased data frequency does increase noise, thus there is a trade-off between a mass flux increase and the data sampling rate. However, there is a real net advantage in signal-to-noise in GC×GC.

It is often stated that an increased signal response of 20 to 50 times is obtained in GC×GC compared with the normal capillary GC experiment. The actual increase in mass flux depends on the peak width in the normal GC analysis, the peak width at the end of the second column in the GC×GC experiment, and the frequency of the modulation. For a response height increase (of the maximum peak pulse), the phase of modulation should also be considered. A number of these factors have been described in the previous section. A peak that is 8 s wide in normal analysis and 150 ms wide in GC×GC will be potentially 50 times taller. This is then moderated by frequency and phase considerations. In a systematic study of sterols by using normal, comprehensive, and targeted GC, the increases in detection limits were reported to be approximately 10 times and 40 times better, respectively, for the latter two methods. The targeted mode fully collected each of the sterol peaks and thus had the best signal enhancement. Lee et al. (26) presented a theoretical study that showed potential improvements in GC×GC analysis (26).

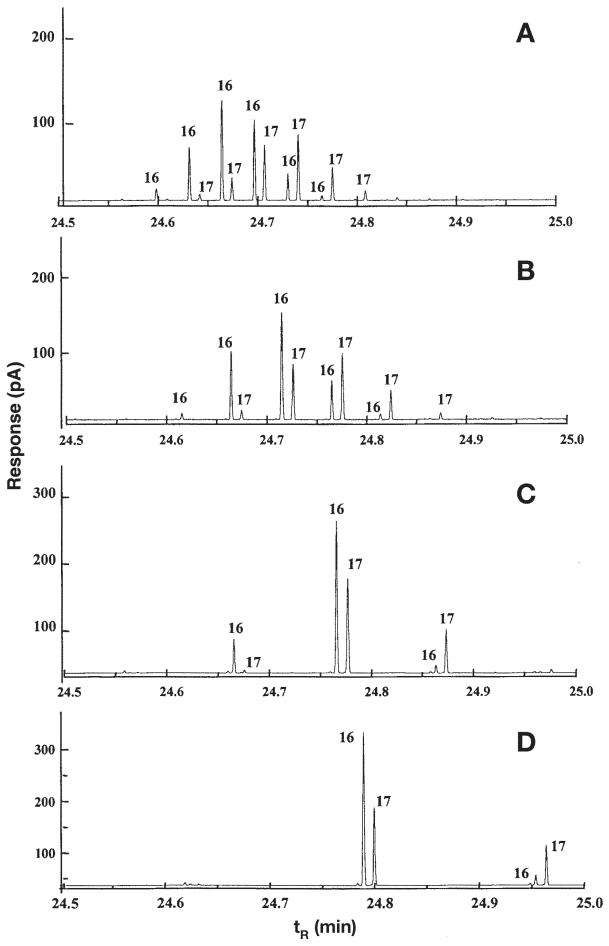

Figure 13. Pulsed peak chromatograms for peaks marked Y in Figure 11. A, B, C, and D are for modulation phases of 2, 3, 6, and 9.9 s, respectively. Peak 16 is the component that elutes earlier than peak 17 in both the first and second dimensions.

It should be noted that sensitivity enhancement is merely with respect to peak response height. There is no improvement in peak areas, because the injected quantity of sample is only dependent on the injection mode. However, the time compression effect does mean that the narrow peaks now have a response that gives a significant signal above the noise level, thus a peak that might not have been seen in conventional GC is now measurable in GC×GC. It is probably recognized that one of the major goals of chromatography over the years has been improved sensitivity, and this is a significant additional (but probably secondary) outcome of GC×GC. It still may be critical in some instances.

Peak capacity increases

If we ask ourselves why there are considerable efforts by a number of research groups put into GC×GC there can be only one answer, and that is the continuing search for greater analytical separation power (apart from the fascinating GC results that are obtained). This is translated into a greater peak capacity over that achieved in single-column analysis. Giddings (7) reported that a comprehensive 2D analysis should be able to produce a total peak capacity equal to that of the product of the capacity of each dimension. Therefore, in a two-column experiment using temperature programming over a period of 60 min, if the first column generates peaks of an average base width of 10 s (in which this constitutes resolved peaks), then this dimension has a total capacity of 600 resolvable peaks. If the second orthogonal column is capable of separating 12 peaks in 3 s (i.e., the average peak base width is 250 ms), then the total available separation space has a peak capacity of 600 × 12 = 7200 peaks (i.e., it is potentially capable of resolving 7200 separate peaks). There is a natural redundancy in as much as some peaks that coelute on the first column may have an insufficient polarity difference to be resolved in the second column, but the purpose of this calculation is to demonstrate that in sheer separation power there is almost an unimaginable opportunity to study complex samples. The only question is the proper choice of column sets to ensure orthogonality. On a purely statistical basis, the extra peak capacity can be directly translated into a greater separation of components. This has been shown time and again in GC×GC applications and has been considered theoretically by Davis (5). Seeley (16) discussed this for a synthetic sample of 100 or more volatile compounds.

Sample analysis by using GC×GC

Effect of sample amount

The role of GC×GC in the analysis of complex samples (i.e., those with a plethora of components) naturally implies that many will be at low levels and others will be major components. Thus, there is a wide diversity of concentration in the one sample. As more components are to be measured, it is increasingly important to have a wider dynamic range of analysis. In GC×GC, if we use a second column of thin film dimensions, there is a question of overloading the column and a subsequent peak broadening of the peak pulses on that column, as described recently (30). This reduces resolution for some instances in which primary column

overlapping peaks are pulsed to the second column and one of these is in much larger quantity. Thus, if a sufficient sample is introduced to the column to enable the analysis of trace constituents, the probability of major component overload is increased. One additional consideration is that compounds are delivered to the second column only once they elute from the primary column, and this will generally be at a temperature at which the component has a relatively low k value (i.e., at a temperature at which it has a reasonably high vapor pressure), which reduces its tendency towards mobile phase overloading. This will help to maintain a constant distribution constant (K) value with different total amounts of sample injected. The role that stationary phase chemistry plays on nonlinear conditions should also be considered. The tendency of compounds to exhibit convex or concave isotherms typical of stationary phase and mobile phase overloading defines the type of peak shape exhibited by the overloaded component. Maximum peak capacity will be ensured only if linear chromatography conditions are observed. The 2D experiment, however, should mean that for certain analyses it is possible to accept a greater degree of overloading than can be tolerated in single-column analysis in some cases.

Analysis of complex samples

It is not the purpose of this review to present an exhaustive account of applications of GC×GC. With the degree of activity in this area it is likely that new applications applying the benefits of GC×GC for a better advantage will continually be introduced. In order to complete the discussion of fundamental concepts, it is necessary to present a selected demonstration of the technology (refer to the reviews by Bertsch (32) and Marriott (33) and the discussions in these works for further specific applications of typical separations). The traditional petrochemical analysis by GC×GC is typified by the work of Beens et al. (34) and Frysinger and Gaines (14).

In our experience, the following sequence represents a possible protocol to use when approaching sample analysis. (*a*) Chromatograph the sample on a column set to define the total analysis time under normal conditions (i.e., without the cryomodulation process). It should be noted that this column set will be any that is currently used in one of the GCs in the laboratory, and usual sets are comprised of BPX5/BP20 or BPX5/BP50 columns. Based on the (likely) components and logical choice of columns, either of these sets may be preferred as an initial choice. (*b*) Repeat the analysis but now with the cryomodulator operating during the region of interest. (*c*) Study the result especially with regard to the degree of resolution of components that are pulsed to the second column. (*d*) If the resolution is insufficient, adjust the experimental conditions to try to achieve better component resolution. Failing that, consider the likely effect of second-column length on the resolution. If this does not give the desired resolution, consider a change of second-column phase or a different column set. (*e*) For some analytical studies, there may be a much more logical stationary phase combination required, rather than those two sets indicated previously. For instance, columns for chiral analysis may be required for enantiomer resolution, or a liquid crystal phase may be better for PCB analysis.

Figure 11 is a representative case of high-resolution 2D GC×GC analysis of a typical sample of semivolatile aromatics. Maximizing the use of the 2D space is the main goal for ensuring the greatest possible number of resolved components in the analysis. It is likely that as more classes of chemical compounds are studied and the effects of the column sets chosen for GC×GC are quantitated, a better use of the available space will be reduced to a more logical process. It is also likely that the enhanced peak capacity will benefit sample pretreatment aspects of the method protocol because more impurities can be accommodated within the 2D space without compromising the analysis of the target analytes. This should mean that the number of sample-handling steps should be reduced and recovery improved.

It should be noted that other chromatographic dimensions may be coupled comprehensively, as discussed in a reasonably thorough review by Liu and Lee (35), and this potentially extends comprehensive separations to a wider range of solutes.

Conclusion

This review has sought to present fundamental considerations in the GC×GC technique, its implementation, and supporting technologies that are specific to GC×GC. There will be a new thought process required on the part of the chromatographer with respect to interpreting GC×GC results, and especially the need to think in two dimensions.

This study has also reported details of experimental correlations of pulsing duration and the modulation phase with pulsed peak presentation in GC×GC. The phase of the modulation, with respect to the input distribution of a solute entering the modulating cryogenic trap, alters the pulsed peak presentation of data, particularly with respect to the symmetry of the series of peaks generated at the detector. An in-phase and 180° out-of-phase modulation process leads to a symmetric series of peaks, but of a different overall type with the former giving a single maximum and the latter two equal maxima. The larger the pulse duration, then the greater is the chance of variation occurring in the t_R of the largest pulsed peak compared with the expected retention of the peak. The peak maximum response is largest for a larger modulation duration (consistent with a larger amount of solute being zone compressed), but this also depends on the modulation phase. Too great a modulation period leads to deterioration in the resolution of neighboring peaks in a 2D contour data representation. Also, there is a concern for deterioration in the separation of peaks obtained in the first dimension when the contour plot is presented. In a multicomponent sample it is likely that different peaks will exhibit different modulation phases, thus their pulsed peak profiles will be of varying symmetries. This will affect the relative relationship between the peak maxima and the area of individual solutes found for different components in the sample. However, the total peak area will be independent of the modulation phase, thus the peak area should be the most appropriate quantitative measure of response.

The key benefits that GC×GC offers both complex and simple sample mixture analysis cannot be simply dismissed as an interesting but impractical technique. The general observation of sensitivity and peak resolution improvement is clearly available to all sample applications, and the general approach to analyzing samples by using GC×GC is logical. The instrumentation is capable of

operating routinely and reliably with excellent precision of analysis. The future of MDGC separations has never been so promising as it is today.

References

1. J.B. Phillips and J. Beens. *J. Chromatogr. A* **856:** 331–47 (1999).
2. H.-J. de Geus, J. de Boer, J.B. Phillips, E.B. Ledford, Jr., and U.A.T. Brinkman. *J. High Resolut. Chromatogr.* **21:** 411–13 (1998).
3. T.T. Truong, P.J. Marriott, and N.A. Porter. *JAOAC* **84:** 323–35 (2001).
4. P. Marriott, R. Shellie, J. Fergeus, R. Ong, and P. Morrison. *Frag. Flav. J.* **15:** 225–39 (2000).
5. J.M. Davis and C. Samuel. *J. High Resolut. Chromatogr.* **23:** 235–44 (2000).
6. Z. Liu and J.B. Phillips. Comprehensive two-dimensional gas chromatography using an on-column thermal modulator interface. *J. Chromatogr. Sci.* **29:** 227–31 (1991).
7. J.C. Giddings. *Anal. Chem.* **56:** 1258A–70A (1984).
8. G. Schomburg. *LC-GC* **5:** 304–17 (1987).
9. A.L. Lee, A.C. Lewis, K.D. Bartle, J.B. McQuaid, and P.J. Marriott. *J. Microcol. Sep.* **12:** 187–93 (2000).
10. J.B. Phillips and E.B. Ledford. *Field Anal. Chem.* **1:** 23–29 (1996).
11. J.B. Phillips, R.B. Gaines, J. Blomberg, F.W.M. van der Wielen, J.-M. Dimandja, V. Green, J. Granger, D. Patterson, L. Racovalis, H.-J. de Geus, J. de Boer, P. Haglund, J. Lipsky, V. Sinha, and E.B. Ledford. *J. High Resolut. Chromatogr.* **22:** 3–10 (1999).
12. J. Beens, M. Adahchour, R. Vreuls, K. Altena, and U. Brinkman. *J. Chromatogr. A* **919:** 127–32 (2001).
13. E.B. Ledford and C.A. Billesbach. *J. High Resolut. Chromatogr.* **23:** 202–204 (2000).
14. G.S. Frysinger and R.B. Gaines. *J. High Resolut. Chromatogr.* **24:** 87–96 (2001).
15. C.A. Bruckner, B.J. Prazen, and R.E. Synovec. *Anal. Chem.* **70:** 2796–2804 (1998).
16. J.V. Seeley, F. Kramp, and C.J. Hicks. *Anal. Chem.* **72:** 4346–52 (2000).
17. P.J. Marriott. "Orthogonal GC-GC". In *Multidimensional Gas Chromatography*. L. Mondello, A.C. Lewis, and K.D. Bartle, Eds. John Wiley & Sons, Ltd., Chichester, U.K., 2002.
18. P. Haglund, M. Harju, R. Ong, and P. Marriott. *J. Microcol. Sep.* **13(7):** 306–11 (2001).
19. A.C. Lewis, N. Carslaw, P.J. Marriott, R.M. Kinghorn, P. Morrison, A.L. Lee, K.D. Bartle, and M.J. Pilling. *Nature* **405:** 778–81 (2000).
20. R. Western, P. Marriott, and G. Sharp. Presented at the 24th International Symposium on Capillary and Electrophoresis Chromatography, Las Vegas, NV, 2001.
21. G. Frysinger and R. Gaines. *J. High Resolut. Chromatogr.* **22:** 196–200 (1999).
22. R. Shellie, P. Marriott, and P. Morrison. *Anal. Chem.* **73:** 1336–44 (2001).
23. M. van Deursen, J. Beens, J. Reijenga, P. Lipman, and C. Cramers. *J. High. Resol. Chromatogr.* **23:** 507–10 (2000).
24. R. Murphy, M. Schure, and J. Foley. *Anal. Chem.* **70:** 1585–94 (1998).
25. J. Beens, H. Boelens, R. Tijssen, and J. Blomberg. *J. High Resolut. Chromatogr.* **21:** 47–54 (1998).
26. A.L. Lee, K.D. Bartle, and A.C. Lewis. *Anal. Chem.* **73:** 1330–35 (2001).
27. R.M. Kinghorn and P.J. Marriott. *Anal. Sci.* **14:** 651–60 (1998).
28. R.M. Kinghorn, P.J. Marriott, and P.A. Dawes. *J. High Resolut. Chromatogr.* **23:** 245–52 (2000).
29. L. Ott and W. Mendenhall. In *Understanding Statistics*. M. Payne, Ed. Duxbury Press, Belmont, CA, 1994.
30. R. Ong, R. Shellie, and P. Marriott. *J. Sep. Sci.* **24:** 367–77 (2001).
31. P.J. Marriott, R.M. Kinghorn, R. Ong, P. Morrison, P. Haglund, and M. Harju. *J. High Resolut. Chromatogr.* **23:** 253–258 (2000).
32. W. Bertsch. *J. High Resolut. Chromatogr.* **23:** 167–81 (2000).
33. P.J. Marriott and R.M. Kinghorn. "Multidimensional and Comprehensive Multidimensional Gas Chromatography: Methods, Applications and Potential". In *Gas Chromatographic Techniques and Applications*. A.J. Handley and E.R. Adlard, Eds. Sheffield Academic Press, Sheffield, U.K., 2001, pp. 260–97.
34. J. Beens, J. Blomberg, and P. Schoenmakers. *J. High Resolut. Chromatogr.* **23:** 182–88 (2000).
35. Z. Liu and M.L. Lee. *J. Microcol. Sep.* **12:** 241–54 (2000).

Manuscript accepted January 8, 2002.